International Journal of Pressure Vessels and Piping 87 (2010) 220–229

Contents lists available at ScienceDirect

International Journal of Pressure Vessels and Piping

journal homepage: www.elsevier.com/locate/ijpvp

A multi-point univariate decomposition method for structural reliability analysis

D. Wei [a], S. Rahman [b,*]

[a] Caterpillar Technical Center, Mossville, IL 61552, USA
[b] Department of Mechanical & Industrial Engineering, The University of Iowa, Iowa City, IA 52242, USA

ARTICLE INFO

Article history:
Received 13 December 2008
Received in revised form
12 March 2010
Accepted 24 March 2010

Keywords:
Multiple most probable points
Design point
Beta point
Reliability
Probability of failure
Decomposition method
Univariate method
FORM/SORM
Monte Carlo simulation

ABSTRACT

A new multi-point univariate decomposition method is presented for structural reliability analysis involving multiple most probable points (MPPs). The method involves a novel function decomposition at all MPPs that facilitates local univariate approximations of a performance function in the rotated Gaussian space, Lagrange interpolation for univariate component functions and return mapping to the standard Gaussian space, and Monte Carlo simulation. In addition to the effort in identifying all MPPs, the computational effort in the multi-point univariate method can be viewed as performing deterministic response analysis at user-selected input defined by sample points. Compared with the existing multi-point FORM/SORM, the multi-point univariate method developed provides a higher-order approximation of the boundary of the failure domain. Both the point-fitted SORM and the univariate method entail linearly varying cost with respect to the number of variables. However, the univariate method with less than nine sample points requires fewer calculations of the performance function than the point-fitted SORM. Numerical results indicate that the proposed method consistently generates an accurate and computationally efficient estimate of the probability of failure.

Published by Elsevier Ltd.

1. Introduction

Structural reliability analysis frequently involves calculation of a component probability of failure

$$P_F \equiv P[g(\mathbf{X}) < 0] = \int_{g(\mathbf{x})<0} f_{\mathbf{X}}(\mathbf{x})d\mathbf{x}, \quad (1)$$

where $\mathbf{X} = \{X_1, \ldots, X_N\}^T \in \mathbb{R}^N$ is a real N-dimensional random vector defined on a probability space $(\Omega, \mathcal{F}, P)$ comprising the sample space Ω, the σ-field $\mathcal{F}$, and the probability measure P; $g : \mathbb{R}^N \to \mathbb{R}$ is a performance function, such that $\Omega_F \equiv \{\mathbf{x} : g(\mathbf{x}) < 0\}$ represents the failure domain; and $f_{\mathbf{X}} : \mathbb{R}^N \to \mathbb{R}$ is the joint probability density function of $\boldsymbol{X}$, which typically represents loads, material properties, and geometry. The most common approach to compute the failure probability in Equation (1) involves the first- and second-order reliability methods (FORM/SORM) [1–3], which are respectively based on linear (FORM) and quadratic (SORM) approximations of the limit-state surface at a most probable point (MPP) in the standard Gaussian space. When the distance β between the origin and MPP (a point on the limit-state surface that is closest to the origin), known as the Hasofer-Lind reliability index, approaches infinity, FORM/SORM provide strictly asymptotic solutions. For non-asymptotic (finite β) applications involving a highly nonlinear performance function, its linear or quadratic approximation may not be adequate and, therefore, resultant FORM/SORM predictions should be interpreted with caution [4,5]. In latter cases, an importance sampling method developed by Hohenbichler and Rackwitz [6] can make FORM/SORM result arbitrarily exact, but it may become expensive if a large number of costly numerical analysis, such as large-scale finite element analysis embedded in the performance function, are involved. In addition, if multiple MPPs exist in either asymptotic or non-asymptotic applications, or if there are contributions from other regions around local minima besides the region around a single MPP, classical FORM/SORM may yield erroneous estimates of the failure probability [7–10]. Therefore, methods that can account for both sources of errors due to high nonlinearity and multiple MPPs are required for structural reliability analysis.

For reliability problems entailing multiple MPPs, the failure probability can be estimated by the multi-point FORM/SORM, which leads to a probability of the union of approximate events [3]. Der Kiureghian and Dakessian [7] proposed a so-called “barrier” method to successively find multiple MPPs. Subsequently, FORM/SORM approximations at each MPP followed by a series system reliability analysis were employed to estimate the failure probability. While the multi-point FORM/SORM account for all MPPs, the resultant effects are limited to first- or second-order approximations of the

* Corresponding author. Tel.: +1 319 335 5679; fax: +1 319 335 5669.
E-mail address: rahman@engineering.uiowa.edu (S. Rahman).

0308-0161/$ – see front matter Published by Elsevier Ltd.
doi:10.1016/j.ijpvp.2010.03.021

performance function. More recently, Au et al. [8] presented asymptotic approximations and importance sampling methods for solving reliability problems with multiple MPPs. Mahadevan and Shi [9] proposed a multiple linearization method in which the limit-state surface is approximated using multiple linear hyperplanes. However, for a general reliability analysis involving a large number of random variables, it is difficult to determine the number of linearization points and locate them systematically. Gupta and Manohar [10] proposed a global response surface method, which constructs a response surface of the limit state by using the global information, rather than the local information around a single MPP. This method requires defining a new set of coordinates and a number of shifting origins in advance. If the performance function is implicit and/or the number of random variables is very large, it is difficult to apply this strategy. Recently, the authors have developed a new class of reliability methods, called the mean- [5] and MPP-based [11,12] dimensional decomposition methods, which are based on a finite hierarchical expansion of the performance function in terms of input variables with increasing dimension. Although these decomposition methods provide higher-order approximations of a performance function, they cannot account for multiple MPPs [11,12]. Hence, developing a multi-point decomposition method in the spirit of the multi-point FORM/SORM that accounts for high nonlinearity and multiple MPPs is the principal motivation of this work.

This paper presents a new multi-point univariate decomposition method for predicting component reliability of mechanical systems subject to random loads, material properties, and geometry. Section 2 gives a brief exposition of novel function decomposition at an MPP that facilitates a lower-dimensional approximation of a general multivariate function. Section 3 describes the proposed univariate method that involves local univariate approximations of the performance function with multiple MPPs, Lagrange interpolation of univariate component functions, return mapping, and Monte Carlo simulation. The section also explains the computational effort and flowchart of the proposed method. Three numerical examples involving elementary mathematical functions and a structural dynamics problem illustrate the method developed in Section 4. Finally, Section 5 provides conclusions from this work.

2. Performance function decomposition at the *m*th MPP

Consider a continuous, differentiable, real-valued performance function $g(\mathbf{x})$ that depends on $\mathbf{x} = \{x_1, \ldots, x_N\}^T \in \mathbb{R}^N$. The transformed limit state $h(\mathbf{u}) = 0$ is the map of $g(\mathbf{x}) = 0$ in the standard Gaussian space ($\mathbf{u}$ space), as shown in Fig. 1 for $N = 2$. Let the performance function contain M number of MPPs $\mathbf{u}_1^*, \ldots, \mathbf{u}_M^*$ with corresponding distances $\beta_1, \ldots, \beta_M$ (Fig. 1).

For the mth MPP, define an associated local coordinate system $\mathbf{v}_m = \{v_{m,1}, \ldots, v_{m,N}\}$, where $v_{m,N}$ is the coordinate in the direction of the MPP, as depicted in Fig. 1. In the $\mathbf{v}_m$ space, denote the mth MPP by $\mathbf{v}_m^* = \{0, \ldots, 0, \beta_m\}$ and the limit state surface by $y_m(\mathbf{v}_m) = 0$, which is also a map of the original limit state surface $g(\mathbf{x}) = 0$. The decomposition of a general multivariate function $y_m(\mathbf{v}_m)$, described by [11–17]

$$y_m(\mathbf{v}_m) = \underbrace{\underbrace{y_{m,0} + \sum_{i=1}^{N} y_{m,i}(v_{m,i})}_{=\widehat{y}_{m,1}(\mathbf{v}_m)} + \sum_{\substack{i_1,i_2=1 \\ i_1<i_2}}^{N} y_{m,i_1 i_2}(v_{m,i_1}, v_{m,i_2})}_{=\widehat{y}_{m,2}(\mathbf{v}_m)} + \ldots + y_{m,12\ldots N}(v_{m,1}, \ldots, v_{m,N}), \tag{2}$$

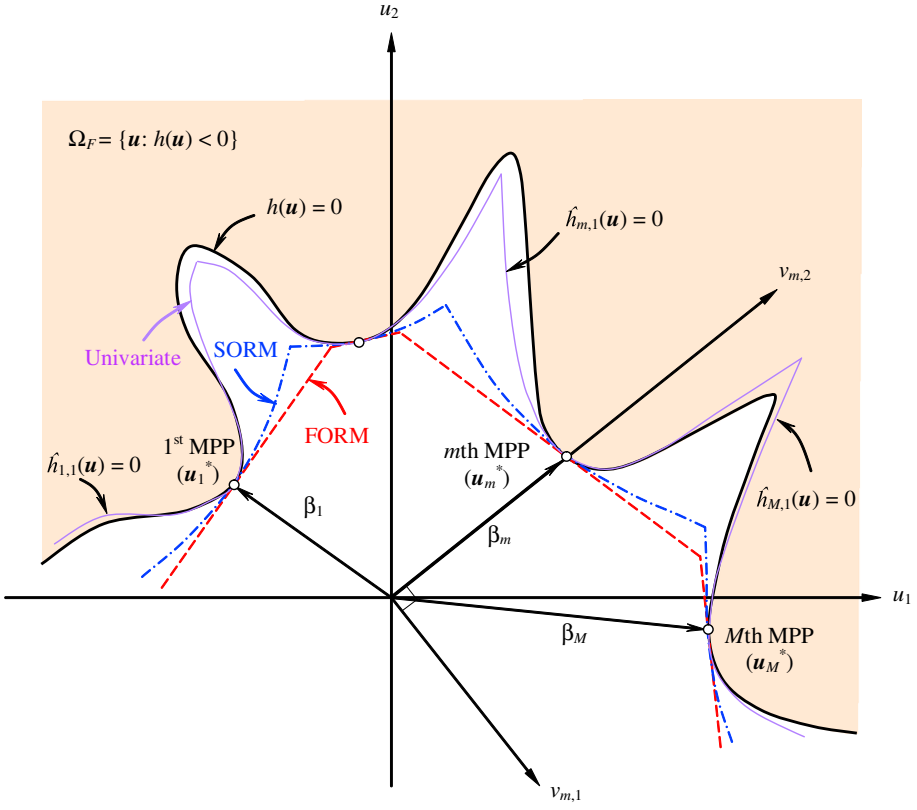

Fig. 1. A performance function with multiple most probable points.

can be viewed as a finite hierarchical expansion of an output function in terms of its input variables with increasing dimension, where $y_{m,0}$ is a constant, $y_{m,i}(v_{m,i}) : \mathbb{R} \mapsto \mathbb{R}$ is a univariate component function representing individual contribution to $y_m(\mathbf{v}_m)$ by input variable $v_{m,i}$ acting alone, $y_{m,i_1 i_2}(v_{m,i_1}, v_{m,i_2}) : \mathbb{R}^2 \mapsto \mathbb{R}$ is a bivariate component function describing cooperative influence of two input variables v_{m,i_1} and v_{m,i_2}, and so on. If

$$\widehat{y}_{m,S}(\mathbf{v}_m) = y_{m,0} + \sum_{i=1}^{N} y_{m,i}(v_{m,i}) + \sum_{\substack{i_1,i_2=1 \\ i_1<i_2}}^{N} y_{m,i_1 i_2}(v_{m,i_1}, v_{m,i_2}) + \ldots + \sum_{\substack{i_1,\ldots,i_S=1 \\ i_1<\ldots<i_S}}^{N} y_{m,i_1\ldots i_S}(v_{m,i_1}, \ldots, v_{m,i_S}) \tag{3}$$

represents a general S-variate approximation of $y_m(\mathbf{v}_m)$, the univariate $(S=1)$ approximation $\widehat{y}_{m,1}(\mathbf{v}_m)$ provides a two-term approximant of the finite decomposition in Equation (2). Similarly, bivariate, trivariate, and other higher-variate approximations can be derived by appropriately selecting the value of S. The fundamental conjecture underlying this work is that component functions arising in the function decomposition will exhibit insignificant S-variate effects cooperatively when $S \to N$, leading to useful lower-variate approximations of $y_m(\mathbf{v}_m)$ [11–17]. In the limit, when $S = N$, $\widehat{y}_{m,N}(\mathbf{v}_m)$ converges to the exact function $y_m(\mathbf{v}_m)$. In other words, Equation (3) generates a hierarchical and convergent sequence of approximations of $y_m(\mathbf{v}_m)$.

The decomposition presented in Equation (2) is well known in the statistics literature as Analysis of Variance (ANOVA) [13]. This decomposition, later referred to as high-dimensional model representation (HDMR) by Rabitz's group, was subject to further refinement leading to notable contributions in function approximations, including the ANOVA-HDMR [14], Cut-HDMR [15], and random sampling (RS)-HDMR [16]. Readers interested in the fundamental details of the decomposition method are referred to authors' past work [17].

3. Multi-point univariate decomposition method

3.1. Univariate decomposition of performance function

At the mth MPP, consider a univariate $(S=1)$ approximation of $y_m(\mathbf{v}_m)$, denoted by

$$\begin{aligned}\widehat{y}_{m,1}(\mathbf{v}_m) &\equiv \widehat{y}_{m,1}(v_{m,1}, \ldots, v_{m,N}) \\ &= \sum_{i=1}^{N} y_m(0, \ldots, 0, v_{m,i}, 0, \ldots, \beta_m) - (N-1) y_m(\mathbf{v}_m^*) \\ &= \sum_{i=1}^{N} \underbrace{y_m(0, \ldots, 0, v_{m,i}, 0, \ldots, \beta_m)}_{= y_{m,i}(v_{m,i})},\end{aligned} \tag{4}$$

where $y_m(\mathbf{v}_m^*) \equiv y_m(0, \ldots, 0, \beta_m) = 0$ and $y_{m,i}(v_{m,i}) \equiv y_m(0, \ldots, 0, v_{m,i}, 0, \ldots, \beta_m)$. Using a multivariate function theorem [17], it can be shown that the univariate approximation $\widehat{y}_{m,1}(\mathbf{v}_m)$ leads to the residual error $y_m(\mathbf{v}_m) - \widehat{y}_{m,1}(\mathbf{v}_m)$, which includes contributions from terms of dimension two and higher. For a sufficiently smooth $y_m(\mathbf{v}_m)$ with a convergent Taylor series, the coefficients associated with higher-dimensional terms are usually much smaller than that with one-dimensional terms. As such, higher-dimensional terms contribute less to the function, and therefore, can be neglected. Nevertheless, Equation (4) includes all higher-order *univariate* terms. In contrast, FORM entails a univariate approximation retaining only *linear* terms. Hence, Equation (4) should provide in general a higher-order approximation of the performance function than FORM. The curvature-fitted SORM [18] has cross-terms, but is limited to a *quadratic* approximation. The errors in neglecting the cross terms, already quantified by Der Kiureghian et al. [19] for various selections of the rotation matrix, are not alarming, and led to the development of the point-fitted SORM. If, indeed, the second-order cross-terms are negligibly small, then the univariate decomposition may also provide a better approximation than SORM. Otherwise, a bivariate or higher-variate decomposition may be required, but they are computationally demanding [5].

3.2. Lagrange interpolation and return mapping

Consider the univariate component function $y_{m,i}(v_{m,i}) \equiv y_m(0, \ldots, 0, v_{m,i}, 0, \ldots, \beta_m)$ in Equation (4). If for sample points $v_{m,i} = v_{m,i}^{(j)}; j = 1, \ldots, n$, n function values $A_{mi,j} \equiv y_m(0, \ldots, 0, v_{m,i}^{(j)}, 0, \ldots, \beta_m); j = 1, \ldots, n$, are given, then the function value for an arbitrary $v_{m,i}$ can be obtained by the Lagrange interpolation

$$\begin{aligned}y_{m,i}(v_{m,i}) &= \sum_{j=1}^{n} \phi_j(v_{m,i}) y_m(0, \ldots, 0, v_{m,i}^{(j)}, 0, \ldots, \beta_m) \\ &= \sum_{j=1}^{n} A_{mi,j} \phi_j(v_{m,i}),\end{aligned} \tag{5}$$

where

$$\phi_j(v_{m,i}) = \frac{\prod_{k=1, k\neq j}^{n} \left(v_{m,i} - v_{m,i}^{(k)}\right)}{\prod_{k=1, k\neq j}^{n} \left(v_{m,i}^{(j)} - v_{m,i}^{(k)}\right)} \tag{6}$$

is the shape function. By using Equations (5) and (6), arbitrarily many values of $y_i(v_{m,i})$ can be generated if n values of that component function are given. The same procedure is repeated for all univariate component functions, *i.e.*, for all $y_{m,i}(v_{m,i}), i = 1, \ldots, N$, leading to an explicit univariate approximation

$$\widehat{y}_{m,1}(\mathbf{V}_m) \equiv \sum_{i=1}^{N} \sum_{j=1}^{n} A_{mi,j} \phi_j(V_{m,i}). \tag{7}$$

By developing similar decompositions at all MPPs (*i.e.*, for all $m = 1, \ldots, M$), univariate approximations $\widehat{y}_{1,1}(\mathbf{V}_1), \ldots, \widehat{y}_{M,1}(\mathbf{V}_M)$ associated with M number of MPPs can be generated.

The functions $\widehat{y}_{1,1}(\mathbf{V}_1), \ldots, \widehat{y}_{M,1}(\mathbf{V}_M)$ represent M local approximations in vicinities of MPPs $\mathbf{v}_1^*, \ldots, \mathbf{v}_M^*$ of $\mathbf{v}_1, \ldots, \mathbf{v}_M$ spaces, respectively. To describe these approximations in a common space, such as the $\mathbf{u}$ space, consider a return mapping $\mathbf{u} = \mathbf{R}_m \mathbf{v}_m$, where $\mathbf{R}_m = [R_{m,ik}]; i, k = 1, \ldots, N$, is an $N \times N$ orthogonal rotation matrix associated with the mth MPP. The matrix $\mathbf{R}_m \in \mathbb{R}^{N\times N}$ has its Nth column $\boldsymbol{\alpha}_m^* \equiv \mathbf{u}_m^*/\beta_m$, *i.e.*, $\mathbf{R}_m = [\mathbf{R}_{m,1} | \boldsymbol{\alpha}_m^*]$, where $\mathbf{R}_{m,1} \in \mathbb{R}^{N\times N-1}$, which satisfies $\boldsymbol{\alpha}_m^{*T} \mathbf{R}_{m,1} = \mathbf{0} \in \mathbb{R}^{1\times N-1}$, can be obtained from the Gram-Schmidt orthogonalization. Consequently, M local approximations of the performance function in the $\mathbf{u}$ space result in

$$\widehat{h}_{m,1}(\mathbf{U}) = \sum_{i=1}^{N} \sum_{j=1}^{n} A_{mi,j} \phi_j\left(\sum_{k=1}^{N} R_{m,ki} U_k\right); \quad m = 1, \ldots, M, \tag{8}$$

as schematically depicted in Fig. 1. Therefore, the actual failure domain, defined as

$$\Omega_F \equiv \{\mathbf{x} : g(\mathbf{x}) < 0\} = \{\mathbf{u} : h(\mathbf{u}) < 0\}, \tag{9}$$

and represented by the shaded area in Fig. 1 can be approximated by a union of M failure sub-domains $\hat{h}_{1,1}(\mathbf{u}) < 0, \ldots, \hat{h}_{M,1}(\mathbf{u}) < 0$, thereby yielding the univariate approximation

$$\hat{\Omega}_F = \left\{ \mathbf{u} : \bigcup_{m=1}^{M} \hat{h}_{m,1}(\mathbf{u}) < 0 \right\}. \tag{10}$$

Note that the boundary of the failure domain $\hat{\Omega}_F$ can be highly nonlinear, which depends on how $\hat{y}_{m,1}(\mathbf{v}_m)$ or $\hat{h}_{m,1}(\mathbf{u})$ are constructed. In contrast, FORM/SORM produce only multi-linear or multi-quadratic boundaries, also plotted in Fig. 1. Therefore, the failure domain defined by Equation (10) with a Lagrange interpolation with $n \geq 3$ should provide a higher-order approximation than that by the multi-point FORM/SORM.

It is well known that the number and location of sample points can significantly alter a response surface approximation in a high-dimensional space. But, in the decomposition proposed, the Lagrange interpolations (Equations (5)–(7)) are constructed in one-dimensional space; therefore, the resulting response surface approximation should not be as sensitive as in the N-dimensional space. Nevertheless, the number and location of sample points should be selected in such a way that the resulting univariate approximation is insensitive to further refinement. The authors' experience suggests that a uniform spacing with three to five sample points works well unless the input uncertainty or the nonlinearity of the component function is overly large, in which case a larger number of sample points may be required.

3.3. Monte Carlo simulation

Once the Lagrange shape functions $\phi_j(v_{m,i})$ and deterministic coefficients $A_{mi,j}; j = 1, \ldots, n$, are generated for all $i = 1, \ldots, N$ and $m = 1, \ldots, M$, Equation (8) provides an explicit local approximation of the performance function in terms of the random input $\boldsymbol{U}$. Therefore, any probabilistic characteristics of a response, including its moments and probability density function, can be easily evaluated by performing Monte Carlo simulation on Equation (8). For a component reliability analysis, the Monte Carlo estimate of the failure probability employing the proposed univariate approximation is

$$P_F \cong P\left(\mathbf{U} \in \hat{\Omega}_F\right) \cong \frac{1}{N_S} \sum_{l=1}^{N_S} \mathbb{I}\left[\bigcup_{m=1}^{M} \hat{h}_{m,1}\left(\mathbf{u}^{(l)}\right) < 0 \right], \tag{11}$$

where $\mathbf{u}^{(l)}$ is the lth realization of $\boldsymbol{U}$, N_S is the sample size, and $\mathbb{I}[\cdot]$ is an indicator function such that $\mathbb{I} = 1$ if $\mathbf{u}^{(l)}$ is in the failure set (*i.e.*, when $\mathbf{u}^{(l)} \in \hat{\Omega}_F$) and *zero* otherwise. Since Equations (8) and (10) are explicit and do not require additional numerical evaluations of response (*e.g.*, solving governing equations by expensive finite element analysis), the embedded Monte Carlo simulation can be efficiently conducted for any sample size.

The proposed method involving multi-point univariate approximation, n-point Lagrange interpolation, and Monte Carlo simulation is defined as the *multi-point univariate decomposition method* in this paper. Fig. 2 shows the computational flowchart of the method developed.

3.4. Computational effort

The multi-point univariate decomposition method requires evaluation of coefficients $A_{mi,j} = y_m(0, \ldots, 0, v_{m,i}^{(j)}, 0, \ldots, \beta_m)$; for $j = 1, \ldots, n$; $i = 1, \ldots, N$ and $m = 1, \ldots, M$. Hence, the computational effort required by the proposed method can be viewed as numerically evaluating the original performance function at several deterministic input defined by user-selected sample points. For each

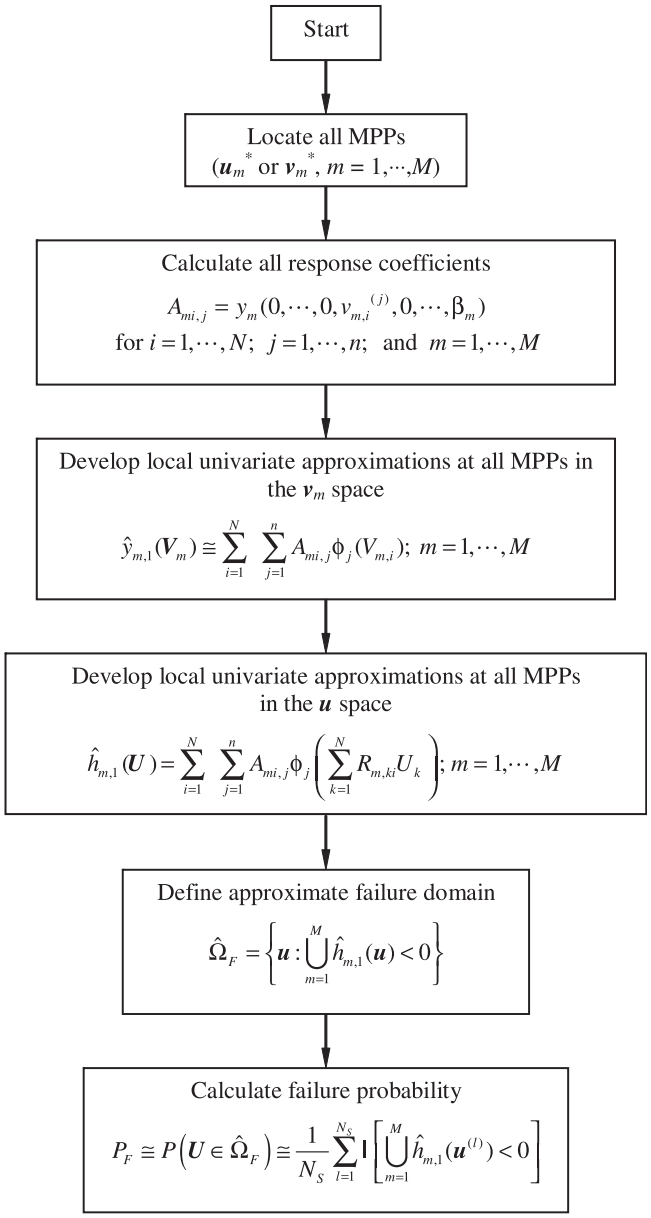

Fig. 2. Flowchart of the multi-point univariate decomposition method.

MPP, there are nN numerical evaluations of $y_m(\mathbf{v}_m)$ involved in Equation (5) for all component functions. Therefore, the total cost entails a *maximum* of $M[nN]$ function evaluations in addition to those required for locating all MPPs. If the sample points include a common point (*e.g.*, MPP) in each coordinate (see the forthcoming section), the total number of function evaluations reduces to $M[(n-1)N]$, *i.e.*, n is replaced with $n-1$.

An important advantage of the univariate decomposition method over SORM is that it requires less computation of the performance function when the number of random variables is large. For a reliability problem with N variables, consider the computational efforts required by the curvature-fitted SORM [18], the point-fitted SORM [19], and the univariate decomposition method in approximating the performance function at a specific MPP. The curvature-fitted SORM for obtaining the Hessian matrix requires $2(N-1)^2$ and $N(N+1)/2$ calculations using the central- and forward-difference schemes, respectively. In addition, with the curvature-fitted SORM, an eigenvalue problem needs to be solved. The quadratic cost scaling in the

curvature-fitted SORM can be significantly reduced by employing the point-fitted SORM, which, assuming four calculations of the performance function per fitting point, requires a total of $8(N-1)$ function evaluations, yielding an alternative second-order approximation without the second-order cross terms [19]. Finally, the number of computations involved in the univariate decomposition method is $N(n-1)$, which also depends on the number of sample points (n). A comparison of computational efforts by these methods, illustrated in Fig. 3, suggests that both the point-fitted SORM and univariate decomposition method entail linearly varying cost, and are therefore significantly more efficient than the curvature-fitted SORM, particularly when N is large. By setting $N(n-1) = 8(N-1)$, $n = 9 - 8/N$, which approaches 9 when $N \to \infty$. Therefore, for high-dimensional reliability problems, the univariate decomposition method with less than nine sample points requires fewer calculations of the performance function than the point-fitted SORM. Typically three to five sample points are adequate, in which case the computational saving from the univariate decomposition is obvious. For example, when $n = 5$, the univariate decomposition method is less expensive than the point-fitted SORM by a factor of two, as $N \to \infty$. When $n = 3$, the cost saving is even larger and nearly four-fold. Furthermore, a selection of $n = 3$ leads to a low-order approximation of the performance function. Therefore, reliability problems with lowly nonlinear performance functions, where quadratic approximations suffice, can be handled by the univariate decomposition method with much less computational effort. Numerical examples (see Examples 2 and 3) presented in the forthcoming section confirm this theoretical observation.

For larger values of n, such as $n \geq 9$, the univariate decomposition method ($N \to \infty$) requires the same or larger number of computations than the point-fitted SORM. However, a large value of n in the univariate decomposition is justified only when the performance function is highly nonlinear – a situation where reliability estimates from second-order approximations may not be adequate.

3.5. Remarks

The multi-point univariate decomposition method is predicated on finding all MPPs that require solving a constrained optimization problem. Existing methods for solving optimization problems for locating all existent MPPs, including the global MPP, are usually heuristic and highly dependent on the nature of the problem being solved. A common approach is to repeat an MPP search with distinct initial points, hoping that all MPPs will be found. Unfortunately, this hardly works, as all trials, depending on the selection of the initial points, may lead to the same MPP, even when other MPPs are present. In this work, a heuristic and robust method, known as the barrier method and developed by Der Kiureghian and Dakessian [7], was employed to find multiple MPPs in the example section. The main idea of the method is to enforce barriers around known MPPs by modifying the performance function and then forcing a standard optimization algorithm – for instance, the Hasofer-Lind-Rackwitz-Fiessler algorithm [20] algorithm – to seek new MPPs. Although the barrier method has worked well for the examples studied, it is important to emphasize that no theoretical proof exists that the method will absolutely find all MPPs for a general reliability problem.

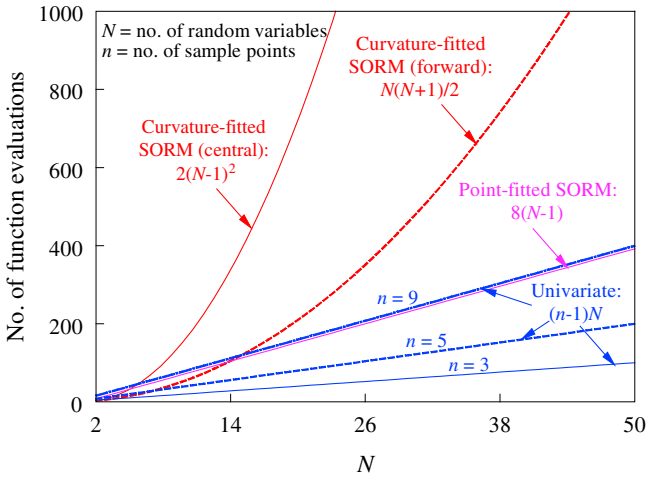

Fig. 3. Computational efforts by SORM and univariate decomposition *method*.

4. Numerical examples

Three numerical examples involving explicit performance functions from mathematical problems (Examples 1 and 2) and an implicit performance function from a structural dynamics problem (Example 3) are presented to illustrate the multi-point univariate decomposition method. Comparisons have been made with existing multi-point FORM/SORM and direct Monte Carlo simulation to evaluate the accuracy and efficiency of the new method. For the multi-point univariate decomposition method, n (=3 or 5) uniformly distributed points $v^*_{m,i} - (n-1)/2, v^*_{m,i} - (n-3)/2, \ldots, v^*_{m,i}, \ldots, v^*_{m,i} + (n-3)/2, v^*_{m,i} + (n-1)/2$ were deployed at the $v_{m,i}$-coordinate of the mth MPP, leading to $M[(n-1)N]$ function evaluations in addition to those required for locating all MPPs. The multi-point FORM/SORM also involved Monte Carlo estimates of the failure probability using their respective approximate failure domains. When comparing computational efforts by various methods, the number of *original* performance function evaluations is selected as the primary metric in this paper.

4.1. Example 1 – mathematical functions with Gaussian random variables

Consider the performance function

$$g(\mathbf{X}) = A + B(X_1 + D)^p - C(X_1 + D)^2 - X_2, \tag{12}$$

where $\mathbf{X} = \{X_1, X_2\}^T \in \mathbb{R}^2$ is a bivariate standard Gaussian random vector with the mean vector $\boldsymbol{\mu}_{\mathbf{X}} \equiv \mathbb{E}[\mathbf{X}] = \mathbf{0} \in \mathbb{R}^2$ and the covariance matrix $\boldsymbol{\Sigma}_{\mathbf{X}} \equiv \mathbb{E}[(\mathbf{X} - \boldsymbol{\mu}_{\mathbf{X}})(\mathbf{X} - \boldsymbol{\mu}_{\mathbf{X}})^T] = \boldsymbol{I} \in \mathbb{R}^{2\times 2}$, where $\boldsymbol{I}$ is the two-dimensional identity matrix; A, B, C, D are real-valued deterministic parameters; and p is an integer-valued deterministic parameter. By appropriately selecting these deterministic parameters, component reliability problems involving a single MPP or multiple MPPs can be constructed. Three cases involving quadratic, cubic, and quartic functions, each containing two MPPs, were studied, as follows.

Case I: $A = 5, B = 0.5, C = 1, D = -0.1, p = 2$ (Quadratic): For Case I, the quadratic limit-state surface has two MPPs: $\mathbf{u}^*_1 = (2.916, 1.036)$ with the Hasofer-Lind reliability index $\beta_1 = 3.094$, and $\mathbf{u}^*_2 = (-2.741, 0.966)$ with the index $\beta_2 = 2.906$, as shown in Fig. 4. The failure probability was estimated by the proposed univariate method ($n = 3$), FORM, curvature- and point-fitted SORM, and direct Monte Carlo simulation (10^6 samples). The results considering either one MPP (single-point) or two MPPs (multi-point) and associated computational efforts are listed in Table 1. Compared with the benchmark result of the Monte Carlo simulation, all single-point methods generate a large amount of error regardless of whether univariate, FORM, and SORM are employed. This is because both MPPs have significant contributions to the failure probability. Therefore, when two MPPs are accounted for, the proposed multi-point univariate method ($P_F \cong 0.00308$) and both variants of the multi-point SORM ($P_F \cong 0.00291$ and 0.00304) yield highly accurate

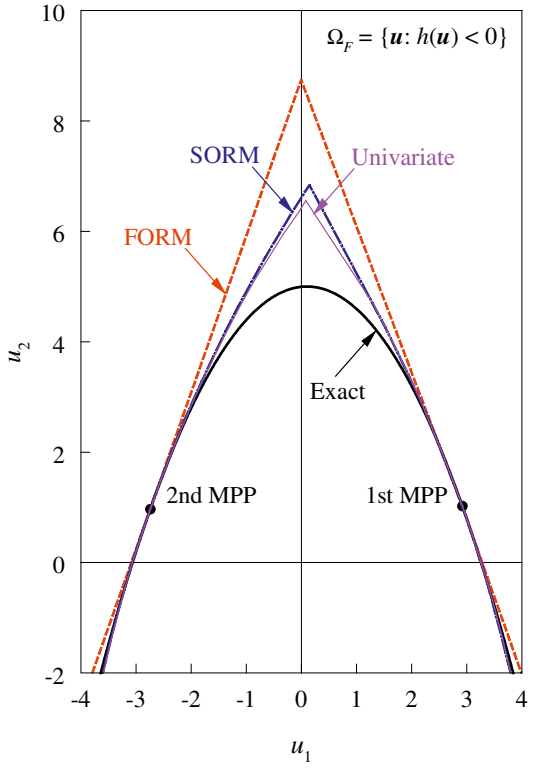

Fig. 4. Quadratic limit-state surface in Case I (Example 1).

results. The multi-point FORM ($P_F \cong 0.00276$), which slightly underpredicts the failure probability, is also fairly accurate. This is because, errors in approximating failure domains by various methods occur far away from the origin. Since the performance function is parabolic, no meaningful difference was observed between the results of the multi-point univariate method and the multi-point SORM. However, a comparison of computational efforts shows slightly or significantly better efficiency of the proposed univariate method when compared with the point-fitted or the curvature-fitted SORM, respectively.

Table 1
Failure probability for quadratic function in Example 1 (Case I).

MPP	Reliability Method	Failure probability	Number of function evaluations[a]
1st MPP ($\boldsymbol{u}_1^*$)	Single-point univariate method	0.00202	45
	Single-point FORM	0.00183	41
	Single-point SORM (curvature-fitted)	0.00195	186
	Single-point SORM (point-fitted)	0.00197	49
2nd MPP ($\boldsymbol{u}_2^*$)	Single-point univariate method	0.00113	50
	Single-point FORM	0.000987	46
	Single-point SORM (curvature-fitted)	0.00106	191
	Single-point SORM (point-fitted)	0.00107	54
Both MPPs ($\boldsymbol{u}_1^*$ and $\boldsymbol{u}_2^*$)	Multi-point univariate method	0.00308	95
	Multi-point FORM	0.00276	87
	Multi-point SORM (curvature-fitted)	0.00291	377
	Multi-point SORM (point-fitted)	0.00304	103
	Direct Monte Carlo simulation	0.00304	1,000,000

[a] Total number of times the original performance function is calculated.

Case II: $A = 5$, $B = 0.5$, $C = 1.5$, $D = 2$, $p = 3$ (Cubic): As shown in Fig. 5, the limit-state surface for Case II also has two MPPs: $\mathbf{u}_1^* = (0, 3)$ with $\beta_1 = 3$, and $\mathbf{u}_2^* = (-3.431, 0.466)$ with $\beta_2 = 3.462$. Table 2 presents similar comparisons of results and computational efforts by various methods stated earlier. For the univariate method, a value of $n = 5$ was selected to capture higher-order terms of the performance function. The results obtained from single-point and multi-point methods show a similar trend as in Case I. However, since the performance function in this case takes on a cubic form, the multi-point SORM no longer predicts highly accurate results as in Case I. Compared with the Monte Carlo simulation (10^6 samples), the multi-point FORM overestimates the failure probability by 132 percent and the multi-point SORM underestimates the failure probability by 9 percent. Since the performance function is a univariate function ($\mathbf{u}$ space) and the first MPP lies on the u_2 axis (*i.e*, no rotation), the single-point univariate approximation at that MPP and the multi-point univariate approximation yield the exact failure domain. Hence, both single-point (first MPP) and multi-point univariate methods predict the same failure probability estimated by the direct Monte Carlo simulation. The multi-point univariate method is more accurate than either variant of the multi-point SORM and requires only a little more computational effort than the multi-point FORM.

Case III: $A = 3$, $B = 2$, $C = 1$, $D = -0.1$, $p = 4$ (Quartic): The final case involves a quartic limit-state function that also has two MPPs, as shown in Fig. 6. The MPPs are: $\mathbf{u}_1^* = (0.544, 2.881)$ with $\beta_1 = 2.932$, and $\mathbf{u}_2^* = (-0.364, 2.877)$ with $\beta_2 = 2.9$. The failure probability estimates by various methods and their computational efforts are listed in Table 3. For the univariate method, a value of $n = 5$ was selected. Due to higher nonlinearity of the performance function in

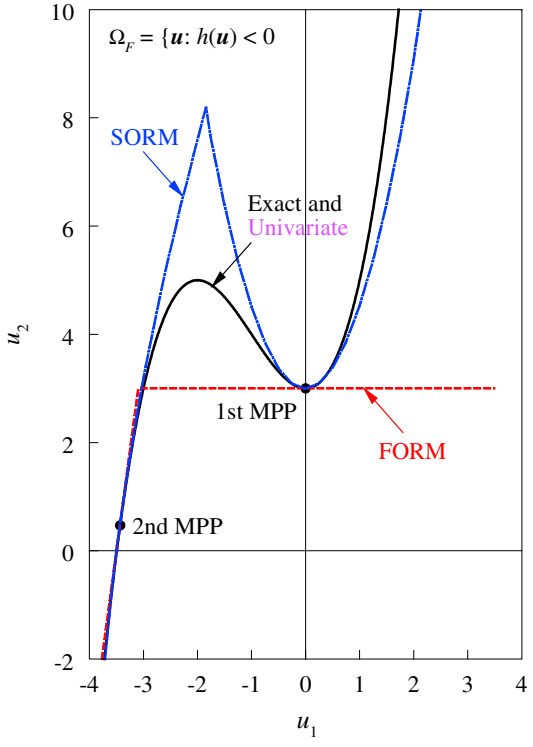

Fig. 5. Cubic limit-state surface in Case II (Example 1).

Table 2
Failure probability for cubic function in Example 1 (Case II).

MPP	Reliability method	Failure probability	Number of function evaluations[a]
1st MPP ($\boldsymbol{u}_1^*$)	Single-point univariate method	0.000721	29
	Single-point FORM	0.00135	21
	Single-point SORM (curvature-fitted)	0.00041	159
	Single-point SORM (point-fitted)	0.00041	29
2nd MPP ($\boldsymbol{u}_2^*$)	Single-point univariate method	0.000276	69
	Single-point FORM	0.000268	61
	Single-point SORM (curvature-fitted)	0.000277	437
	Single-point SORM (point-fitted)	0.000279	69
Both MPPs ($\boldsymbol{u}_1^*$ and $\boldsymbol{u}_2^*$)	Multi-point univariate method	0.000721	98
	Multi-point FORM	0.00167	82
	Multi-point SORM (curvature-fitted)	0.000646	596
	Multi-point SORM (point-fitted)	0.000651	98
	Direct Monte Carlo simulation	0.000721	1,000,000

[a] Total number of times the original performance function is calculated.

Table 3
Failure probability for quartic function in Example 1 (Case III).

MPP	Reliability Method	Failure probability	Number of function evaluations[a]
1st MPP ($\boldsymbol{u}_1^*$)	Single-point univariate method	0.000954	154
	Single-point FORM	0.00169	146
	Single-point SORM (curvature-fitted)	0.000552	439
	Single-point SORM (point-fitted)	0.000519	154
2nd MPP ($\boldsymbol{u}_2^*$)	Single-point univariate method	0.000938	134
	Single-point FORM	0.000186	126
	Single-point SORM (curvature-fitted)	0.000564	259
	Single-point SORM (point-fitted)	0.000527	134
Both MPPs ($\boldsymbol{u}_1^*$ and $\boldsymbol{u}_2^*$)	Multi-point univariate method	0.00101	288
	Multi-point FORM	0.00246	272
	Multi-point SORM (curvature-fitted)	0.00081	698
	Multi-point SORM (point-fitted)	0.000764	288
	Direct Monte Carlo simulation	0.00103	1,000,000

[a] Total number of times the original performance function is calculated.

Case III than that in Cases I and II, the multi-point FORM/SORM fail to provide an accurate solution. Compared with the benchmark result of the Monte Carlo simulation (10^6 samples), the errors in calculating the failure probability by the multi-point FORM and the multi-point SORM are 139 and 23-26 percent, respectively. The multi-point univariate method is more accurate (error ≅ 2 percent) than the multi-point FORM/SORM with a computational effort slightly higher than that required by the multi-point FORM. The higher accuracy of the univariate method is attributed to a higher-order approximation of the failure boundary that permits an accurate representation of the flat region between two MPPs (see Fig. 6). The underprediction of the multi-point SORM is due to its second-order approximation, which cannot capture the flatness of the failure boundary in that region. Although the multi-point FORM approximates that flat region well, it fails to capture the nonlinearity of the performance function on other sides of the MPPs, leading to a significant overprediction of the failure probability. Additional cases entailing higher-order nonlinearity of the performance function can be created in a similar manner to show a progressive loss of accuracy by the multi-point FORM/SORM.

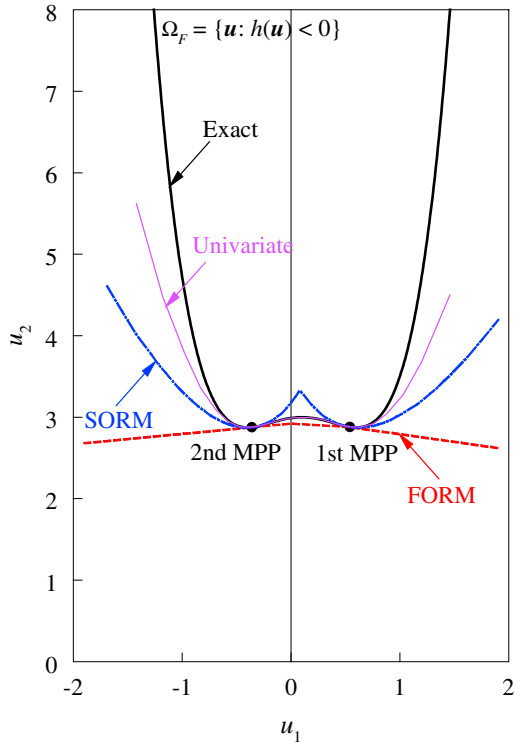

Fig. 6. Quartic limit-state surface in Case III (Example 1).

The results of Cases I-III demonstrate that the multi-point univariate method can consistently handle higher-order reliability problems with multiple MPPs. For all three cases, the boundaries of failure domains plotted in Figs. 4–6 indicate that the univariate method yields a better approximation than FORM/SORM, especially when the performance function is highly nonlinear. The point-fitted multi-point SORM exhibits a similar computational efficiency of the multi-point univariate method, because the analysis performed is only two-dimensional. For higher-dimensional reliability problems, the computational effort by the point-fitted SORM should grow larger than that by the univariate method (see Section 3.4). Nevertheless, the results of the multi-point SORM (curvature- or point-fitted), which captures at most a second-order approximation, should be carefully interpreted when a reliability problem is highly nonlinear.

4.2. Example 2 — mathematical function with Non-Gaussian random variables

A well-known performance function, originally introduced by Hohenbichler and Rackwitz [21] and subsequently discussed by others [1,3,7], is

$$g(\mathbf{X}) = 18 - 3X_1 - 2X_2, \tag{13}$$

where $\mathbf{X} = \{X_1, X_2\}^T \in \mathbb{R}^2$ is a bivariate random vector with the joint cumulative probability distribution function

$$F_{X_1X_2}(x_1,x_2) = \begin{cases} 1-\exp(-x_1)-\exp(-x_2)+\exp[-(x_1+x_2+x_1x_2)], \\ \qquad\qquad x_1,x_2 \geq 0, \\ 0, \qquad\qquad \text{otherwise}. \end{cases} \tag{14}$$

Due to the symmetry in Equation 14 between x_1 and x_2, there are two distinct Rosenblatt transformations [22] depending on the ordering of variables $\{x_1,x_2\}$ and $\{x_2,x_1\}$, which lead to mappings

$$T_1 \equiv (x_1,x_2) \rightarrow (u_1,u_2): \begin{cases} u_1 = \Phi^{-1}\{1-\exp(-x_1)\} \\ u_2 = \Phi^{-1}\{1-(1+x_2)\exp[-x_2(1+x_1)]\} \end{cases} \tag{15}$$

and

$$T_2 \equiv (x_2,x_1) \rightarrow (u_1,u_2): \begin{cases} u_1 = \Phi^{-1}\{1-\exp(-x_2)\} \\ u_2 = \Phi^{-1}\{1-(1+x_1)\exp[-x_1(1+x_2)]\} \end{cases}, \tag{16}$$

respectively, where $\Phi(u) = \int_{-\infty}^{u}(1/\sqrt{2\pi})\exp(-\xi^2/2)d\xi$ is the cumulative distribution function of a standard Gaussian random variable. Due to the nonlinearity of transformations, the linear limit-state surface in the **x** space becomes nonlinear functions in the **u** space, as depicted in Fig. 7(a) and (b) for transformations T_1 and T_2, respectively.

Regardless of the transformation, each limit-state surface possesses two distinct MPPs which are: $\mathbf{u}_1^* = (2.782, 0.0865)$with $\beta_1 = 2.784$, and $\mathbf{u}_2^* = (-1.296, 3.253)$ with $\beta_2 = 3.501$ for transformation T_1; and $\mathbf{u}_1^* = (-1.124, 2.399)$ with $\beta_1 = 2.649$, and $\mathbf{u}_2^* = (3.630, 0.142)$ with $\beta_2 = 3.633$ for transformation T_2. The univariate decomposition method and FORM/SORM entailing single and multiple MPPs were applied to obtain estimates of the failure probability, which are presented in Tables 4 and 5 for transformations T_1 and T_2, respectively. Also listed is the reference solution obtained by the direct Monte Carlo simulation involving 10^6 samples. For the univariate method, a value of $n = 3$ was selected. The tabulated results indicate that the failure probability estimates based on a single MPP strongly depend on the selected transformation and the particular MPP that is found. If an optimization algorithm can find only one (*e.g.*, the second MPP) of these two MPPs, results based on that MPP may contain significant errors regardless of the reliability method employed. The multi-point FORM using the transformation T_1 yields an excellent result, but also produces an erroneous result when the transformation T_2 is chosen. In contrast, the multi-point univariate method and the multi-point curvature-fitted SORM yield excellent estimates of the failure probability regardless of the transformation invoked. The maximum errors by the multi-point univariate method, multi-point FORM, and multi-point SORM are 1.7, 41.2, and 2.7 percent, respectively. Although the univariate method and SORM have comparable accuracies, the multi-point univariate method is more computationally efficient than the multi-point SORM.

4.3. Example 3 — seismic dynamics of a ten-story building-TMD system

In this example, consider a 10-story shear building subjected to seismic ground motion with a tuned mass damper (TMD) placed on the roof, as shown in Fig. 8. This problem, adopted from Der Kiureghian and Dakessian [7], has a slightly different input response spectrum than the one used in the original reference. The building

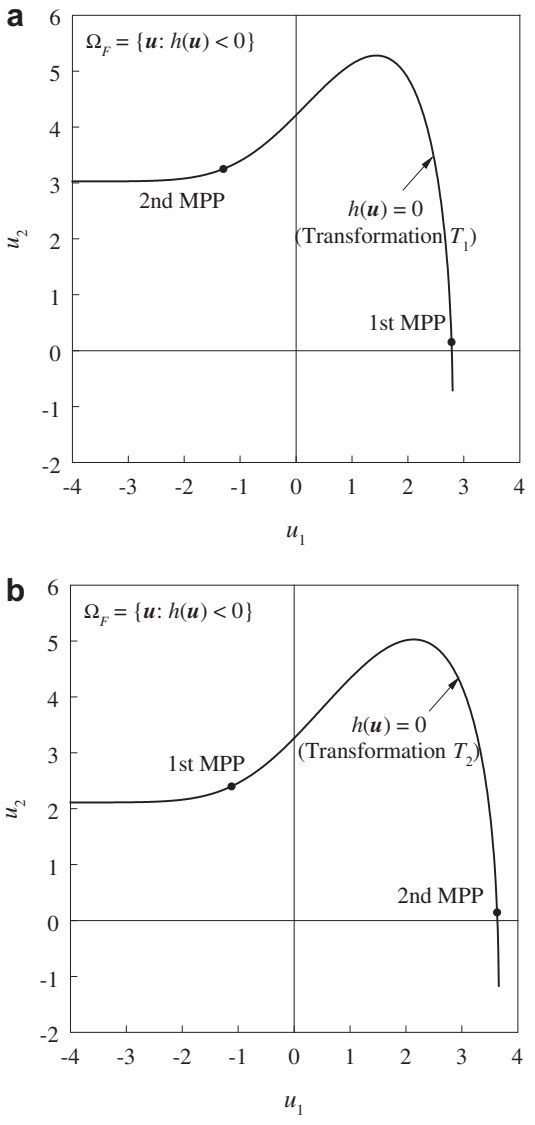

Fig. 7. Limit-state surface of Example 2; (a) transformation T_1; (b) transformation T_2.

Table 4
Failure probability for Example 2 (Transformation T_1).

MPP	Reliability Method	Failure probability	Number of function evaluations[a]
1st MPP ($\boldsymbol{u}_1^*$)	Single-point univariate method	0.00285	45
	Single-point FORM	0.00269	41
	Single-point SORM	0.0028	182
2nd MPP ($\boldsymbol{u}_2^*$)	Single-point univariate method	0.000157	105
	Single-point FORM	0.000232	101
	Single-point SORM	0.000145	244
Both MPPs ($\boldsymbol{u}_1^*$ and $\boldsymbol{u}_2^*$)	Multi-point univariate method	0.00301	150
	Multi-point FORM	0.0029	142
	Multi-point SORM	0.00292	426
	Direct Monte Carlo simulation	0.00296	1,000,000

[a] Total number of times the original performance function is calculated.

Table 5
Failure probability for Example 2 (Transformation T_2).

MPP	Reliability Method	Failure probability	Number of function evaluations[a]
1st MPP ($\boldsymbol{u}_1^*$)	Single-point univariate method	0.00281	85
	Single-point FORM	0.00404	81
	Single-point SORM	0.00273	224
2nd MPP ($\boldsymbol{u}_2^*$)	Single-point univariate method	0.00018	55
	Single-point FORM	0.00014	51
	Single-point SORM	0.00015	196
Both MPPs ($\boldsymbol{u}_1^*$ and $\boldsymbol{u}_2^*$)	Multi-point univariate method	0.00299	140
	Multi-point FORM	0.00417	132
	Multi-point SORM	0.00288	420
	Direct Monte Carlo simulation	0.00296	1,000,000

[a] Total number of times the original performance function is calculated.

has random floor masses $M_i, i = 1,\ldots,10$, and random story stiffness $K_i, i = 1,\ldots,10$. The TMD has a random mass M_0 and random stiffness K_0. The combined system has random modal damping ratios $\zeta_i, i = 0,\ldots,10$. The input motion is defined by a pseudo-acceleration response spectrum $A(T,\zeta) = SH(\zeta)a(T)$, where T is the period, $S = 0.61$ is a scale factor, $H(\zeta)$ is a damping–dependent correction factor defined by the *Applied Technology Council* [23], and $a(T)$ is the pseudo-acceleration response spectrum shape for a 5 percent damping, as shown in Fig. 9. The TMD is effective in reducing the dynamic response of the building over a narrow band of frequencies, providing best results when its natural frequency $\omega_0 = \sqrt{k_0/m_0}$ is perfectly tuned to the fundamental frequency of the building. In reality, due to uncertainties in mass, stiffness, and damping properties, perfect tuning between the TMD and the building may not occur. As a result, the TMD can be over-tuned or under-tuned, leading to two distinct MPPs when conducting reliability analysis of a combined building-TMD system.

For the present reliability analysis, consider the limit-state function

$$g(\mathbf{X}) = V_0 - V_{\text{base}}(\mathbf{X}), \tag{17}$$

where $\mathbf{X} = \{M_0, M_1, \ldots, M_{10}, K_0, K_1, \ldots, K_{10}, \zeta_0, \zeta_1, \ldots, \zeta_{10}\}^T \in \mathbb{R}^{33}$ is a random vector consisting of 33 independent random variables,

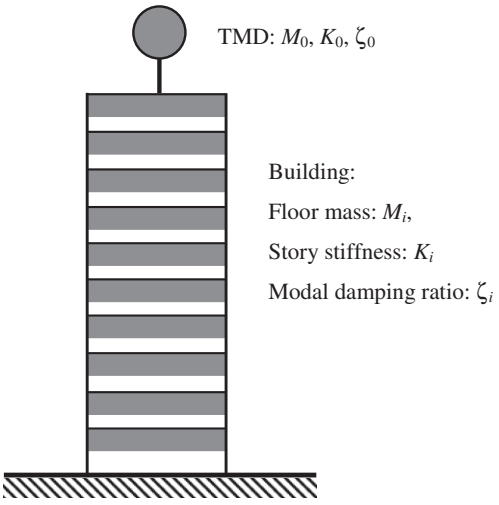

Fig. 8. A ten-story building-TMD system (Example 3).

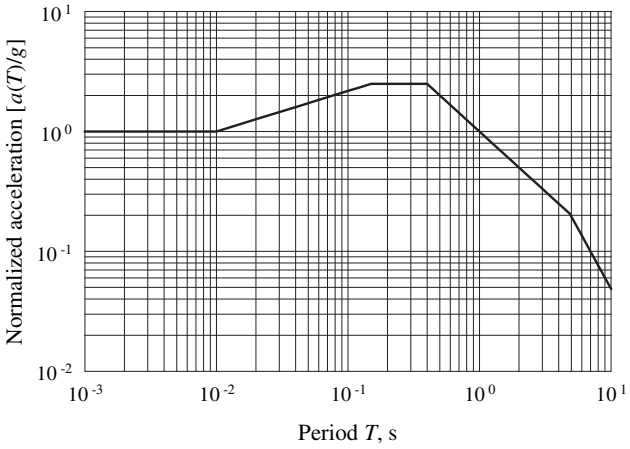

Fig. 9. Normalized pseudo-acceleration response spectrum.

$V_{\text{base}}(\mathbf{X})$ is the base shear response of the building which is an implicit function of $\boldsymbol{X}$, and $V_0 = 1000$ kip is an allowable threshold. Each of these random variable is lognormally distributed with respective means and coefficients of variations listed in Table 6. The base shear is computed by combining modal responses of the 11-DOF building-TMD system using the CQC rule [24]. Each realization of $\boldsymbol{X}$ involves an eigenvalue analysis of the system, the computation of the modal contributions to the base shear, and their combination according to the CQC rule.

Starting from the mean input, the first MPP was found with a value of the Hasofer-Lind reliability index $\beta_1 = 1.137$ (over-tuned). The second MPP was located with the corresponding index $\beta_2 = 1.846$ (under-tuned). Table 7 summarizes various estimates of the failure probability, based on single- and multi-point univariate decomposition methods and FORM/SORM. These results are compared with the solution using the direct Monte Carlo simulation employing 5000 samples. For the univariate method, a value of $n = 3$ was selected. Failure probability estimates by all methods that are based on a single MPP improve when both MPPs are considered. Both the multi-point SORM (curvature-fitted) and multi-point univariate method provide very accurate results. However, by comparing the number of function evaluations, also listed in Table 7, the multi-point univariate decomposition method is more computationally efficient than the multi-point curvature-fitted SORM.

In Examples 2 and 3, the point-fitted SORM is expected to yield results as accurate as those obtained from the curvature-fitted SORM. Therefore, both variants of the multi-point SORM and the multi-point univariate decomposition provide satisfactory estimates of the failure probability in the last two examples. The fundamental reason is that a quadratic approximation of both performance functions is adequate in the vicinity of MPPs. Lowly nonlinear performance functions in the vicinity of MPPs, observed in Fig. 7(a) and (b), explain why the multi-point FORM may also perform well in Example 2. Indeed, the low nonlinearity in Examples 2 and 3 provide the rationale for selecting a low value of n in

Table 6
Statistical properties of random input for Example 3.

Random variable	Mean	Coefficient of variation	Probability distribution
$M_1,\ldots,M_{10}$	193 kip/g	0.2	Lognormal
$K_1,\ldots,K_{10}$	1200 kip/in	0.2	Lognormal
M_0	158 kip/g	0.2	Lognormal
K_0	22 kip/in	0.2	Lognormal
$\zeta_0,\ldots,\zeta_{10}$	0.05	0.3	Lognormal

Table 7
Failure probability for Example 3.

MPP	Reliability method	Failure probability	Number of function evaluations[a]
1st MPP ($\boldsymbol{u}_1^*$)	Single-point univariate method	0.1422	536
	Single-point FORM	0.1278	470
	Single-point SORM	0.1401	1593
2nd MPP ($\boldsymbol{u}_2^*$)	Single-point univariate method	0.0314	737
	Single-point FORM	0.0324	671
	Single-point SORM	0.0295	1794
Both MPPs ($\boldsymbol{u}_1^*$ and $\boldsymbol{u}_2^*$)	Multi-point univariate method	0.163	1273
	Multi-point FORM	0.151	1141
	Multi-point SORM	0.161	3387
	Direct Monte Carlo simulation	0.163	5000

[a] Total number of times the original performance function is calculated.

the univariate decomposition method. Nevertheless, in Example 3 ($N = 33, n = 3$), the total numbers of function evaluations by the proposed method are: (1) 1st MPP: $470(\text{FORM}) + (3-1)\times 33 = 536$; (2) 2nd MPP: $671(\text{FORM}) + (3-1)\times 33 = 737$. In contrast, the point-fitted SORM would have required the following numbers of evaluations: (1) 1st MPP: $470(\text{FORM}) + 8\times(33-1) = 726$; (2) 2nd MPP: $671(\text{FORM}) + 8\times(33-1) = 927$. Therefore, both versions of SORM are more expensive than the proposed univariate method with a low n – a claim supported by Fig. 3 in Section 3.4. The comparison suggests that for lowly nonlinear problems where the multi-point SORM is adequate, the univariate method provides failure probability estimates as accurate as existing methods, but is computationally more efficient than either the curvature- or the point-fitted SORM.

5. Summary and conclusions

A multi-point univariate decomposition method was developed for solving component reliability problems involving multiple most probable points (MPPs). The method is based on: (1) a novel function decomposition at all MPPs that facilitates local univariate approximations of a performance function in the rotated Gaussian space, (2) Lagrange interpolation for univariate component functions and return mapping to the standard Gaussian space, and (3) Monte Carlo simulation. The proposed decomposition results in an approximate failure domain that is constructed by a union of failure sub-domains associated with all MPPs. The boundary of the approximate failure domain can be highly nonlinear, which consists of explicit functions of random input variables. Hence, the embedded Monte Carlo simulation can be conducted for an arbitrarily large sample size. In addition to the effort in identifying all MPPs, the computational effort in the multi-point method developed can be viewed as performing deterministic response analysis at user-selected input defined by sample points. Compared with the multi-point FORM/SORM available in the current literature, the multi-point univariate method provides higher-order approximations of the boundary of the failure domain. Both the point-fitted SORM and the univariate method entail linearly varying cost with respect to the number of variables. However, the univariate method with less than nine sample points requires fewer calculations of the performance function than the point-fitted SORM.

Three numerical examples involving elementary mathematical functions and a structural dynamics problem illustrate the proposed method. Comparisons were made with existing multi-point FORM/SORM and direct Monte Carlo simulation to evaluate the accuracy and computational efficiency of the univariate method developed. Results indicate that the multi-point univariate method consistently provides an accurate and computationally efficient estimate of the probability of failure. For lowly nonlinear problems where the multi-point SORM is adequate, the univariate method provides failure probability estimates as accurate as existing methods, but is computationally more efficient than either the curvature- or the point-fitted SORM.

Acknowledgments

The authors would like to acknowledge financial support from the U.S. National Science Foundation under Grant No. DMI-0355487.

References

[1] Madsen HO, Krenk S, Lind NC. Methods of structural safety. Englewood Cliffs, NJ: Prentice-Hall, Inc.; 1986.
[2] Rackwitz R. Reliability analysis – a review and some perspectives. Structural Safety 2001;23(4):365–95.
[3] Ditlevsen O, Madsen HO. Structural reliability methods. Chichester: John Wiley & Sons Ltd.; 1996.
[4] Nie J, Ellingwood BR. Directional methods for structural reliability analysis. Structural Safety 2000;22:233–49.
[5] Xu H, Rahman S. Decomposition methods for structural reliability analysis. Probabilistic Engineering Mechanics 2005;20:239–50.
[6] Hohenbichler M, Rackwitz R. Improvement of second-order reliability estimates by importance sampling. ASCE Journal of Engineering Mechanics 1988;114(12):2195–8.
[7] Der Kiureghian A, Dakessian T. Multiple design points in first and second-order reliability. Structural Safety 1998;20(1):37–49.
[8] Au SK, Papadimitriou C, Beck JL. Reliability of uncertain dynamical systems with multiple design points. Structural Safety 1999;21:113–33.
[9] Mahadevan S, Shi P. Multiple linearization method for nonlinear reliability analysis. ASCE Journal of Engineering Mechanics 2001;127:1165–73.
[10] Gupta S, Manohar CS. An improved response surface method for the determination of failure probability and importance measures. Structural Safety 2004;26:123–39.
[11] Rahman S, Wei D. A univariate approximation at most probable point for higher-order reliability analysis. International Journal of Solids and Structures 2006;43:2820–39.
[12] Wei D, Rahman S. Structural reliability analysis by univariate decomposition and numerical integration. Probabilistic Engineering Mechanics 2007;22:27–38.
[13] Efron B, Stein C. The Jackknife estimate of variance. Annals of Statistics 1981;9:586–96.
[14] Sobol IM. Theorems and examples on high dimensional model representations. Reliability Engineering and System Safety 2003;79:187–93.
[15] Rabitz H, Alis O. General foundations of high dimensional model representations. Journal of Mathematical Chemistry 1999;25:197–233.
[16] Li G, Wang SW, Rabitz H. Practical approaches to construct RS-HDMR component functions. Journal of Physical Chemistry A 2002;106:8721–33.
[17] Xu H, Rahman S. A generalized dimension-reduction method for multi-dimensional integration in stochastic mechanics. International Journal for Numerical Methods in Engineering 2004;61:1992–2019.
[18] Hohenbichler M, Gollwitzer S, Kruse W, Rackwitz R. New light on first- and second-order reliability methods. Structural Safety 1987;4:267–84.
[19] Der Kiureghian A, Lin H-Z, Hwang S-J. Second-order reliability approximations. ASCE Journal of Engineering Mechanics 1987;113(8):1208–25.
[20] Liu PL, Der Kiureghian A. Optimization algorithms for structural reliability analysis. Report No. UCB/SESM-86/09, Berkeley, CA, 1986.
[21] Hohenbichler M, Rackwitz R. Non-normal dependent vectors in structural safety. ASCE Journal of the Engineering Mechanics Division 1981;107:1227–38.
[22] Rosenblatt M. Remarks on a multivariate transformation. Annals of Mathematical Statistics 1952;23:470–2.
[23] US Army Corps Engineering. Engineering and design – seismic design provisions for roller compacted concrete dams. Report No. EP 1110-2-12, 1995.
[24] Clough RW, Penzien J. Dynamics of structures. 2nd ed. New York, NY: McGraw-Hill, Inc.; 1993.